Physica Scripta. Vol. TXX, 1–7, 2003

Polarization Experiments with Storage Rings

H. O. Meyer[1]

[1] Indiana University, Bloomington, IN 47405, USA

Received June 16, 2002

PACS Ref: 29.20. Dh, 29.25. Pj, 25.10. ts, 25.40. -h; 25.40. Cm, 25.40. Ep.

Abstract

The technical issues are summarized that arise in hadron storage ring experiments with a polarized beam and a polarized internal target. This is followed by a synopsis of polarization experiments in storage rings.

1. Polarized beam in a ring

1.1. *Spin dynamics*

1.1.1. *Spin closed orbit*

The magnetic moments of particles stored in a ring precess around the fields they encounter along their orbit. If the particles are polarized their polarization vector precesses accordingly. This spin motion must repeat on each revolution. For any point along the beam, this condition defines a stable polarization direction, called the *spin closed orbit*. If there are fields other than the bending field, and one knows them, one can calculate the spin closed orbit. This is an eigenvalue problem that is best solved by representing rotations as unitary, complex 2×2 matrices (one of the few classical applications of the SU(2) formalism). A clear account of this topic has been given by Montaigue [1].

The ring environment determines most beam properties. Their values before injection into the ring are lost. This is true for energy, time structure and emittance, but also for the polarization direction: any initial polarization component that is not along the spin closed orbit is quickly washed out. If the field integral around the ring is vertical, the spin closed orbit is vertical everywhere, but spin rotators (so-called snakes) can be used to produce non-vertical spin orientation. A longitudinal solenoid field is an example of a spin rotator.

It is interesting that polarization, in principle, can be transferred from a polarized, internal target to the stored beam [2,3]. This is a small effect that can be observed only because it accumulates as the beam passes through the target many times.

1.1.2. *Resonances*

In a machine where the average field is vertical, the magnetic moments of the beam particles in the particle frame precess with a frequency $f_{orb}G\gamma$, where f_{orb} is the orbit frequency, is the Lorentz factor, and $G = 1/2(g-2)$ follows from the g-factor (for protons, $G_p = 1.79285$). Depolarizing spin resonances arise when this precession is consonant with the particle motion. So-called *imperfection* resonances occur at energies for which G has an integer value. *Intrinsic* resonances are caused by the focusing fields and depend on the vertical and horizontal machine tunes $_v$ and $_h$. They occur when $G = n + m\ _h + k\ _v$ (n, m, k are integers). Finally, *induced* resonances are produced by longitudinal or transverse oscillating fields when the frequency f_{osc} satisfies $f_{osc} = f_{orb}(m + nG)$.

1.2. *Stored polarized protons*

1.2.1. *Polarization reversal*

Crossing a spin resonance at slow speed (adiabatic passage) causes the spin closed orbit to flip by 180°. It has been demonstrated [4–6] that the crossing of an induced resonance (by varying the rf frequency) flips the sign of the polarization (transverse as well as longitudinal) of protons with better than a few percent loss in polarization. This can be an important tool in eliminating systematic errors in polarization experiments.

1.2.2. *Polarization lifetime*

Near a resonance, the spin closed orbit deviates from its off-resonance value and becomes sensitive to the tune and the betatron amplitude, which can be slightly different for individual particles. Thus, the ensemble de-coheres and polarization is lost. This process is not understood in detail but it is still possible to predict the polarization lifetime as a function of the "distance" to the resonance (for an intrinsic resonance, that would be the difference between the actual and the resonant tune). The polarization lifetime for protons has been measured near an intrinsic resonance [7] and an induced resonance [8].

One finds that the effect of a resonance is very localized. Thus, the polarization of a stored beam is remarkably stable, and if one is not extremely close to a resonance the polarization lifetime is much longer than the beam intensity lifetime.

1.2.3. *Acceleration of polarized beam*

In the absence of resonances, changing the energy of the beam hardly affects its polarization. This was demonstrated by measuring the polarization of a 200 MeV beam, accelerating it to 450 MeV, decelerating back to 200 MeV, and repeating the polarization measurement [9]. This persistence of polarization makes it possible to export a *polarization standard* (a known analyzing power at a given energy) to any other energy that can be reached by accelerating or decelerating the stored beam.

When accelerating the beam to higher energies, eventually depolarizing resonances have to be crossed. In order to preserve the polarization, imperfection resonances may be enhanced to affect a *complete* spin flip [10], while a sudden tune change may be used to *jump* over intrinsic resonances (as is done at COSY). Another method to avoid depolarizing resonances involves the use of spin rotators

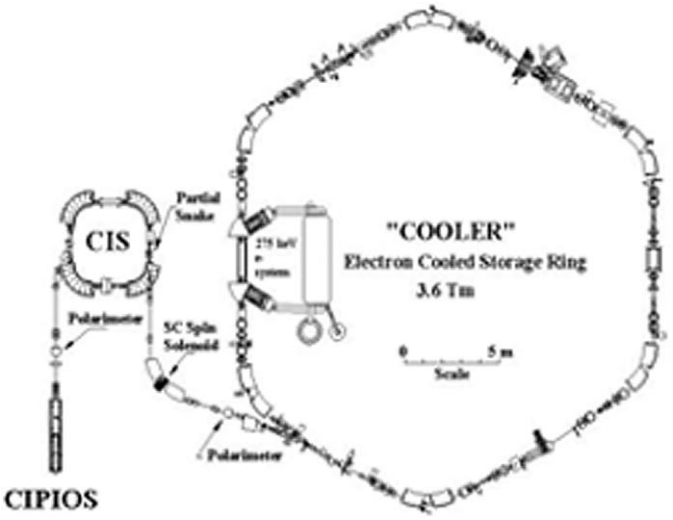

Fig. 1 The Indiana Cooler, 1988–2002.

(so-called Siberian snakes). The effectiveness of such a device has been demonstrated for the first time at the Indiana Cooler [11,12] (see Fig. 1). At this time, RHIC is operating a multitude of snakes to preserve beam polarization up to 500 GeV.

1.3. *Stored polarized deuterons*

1.3.1. *Polarization of spin-1 particles*

While the three components of the polarization vector are sufficient to describe an ensemble of spin-1/2 protons, eight real numbers are in general required for spin-1 deuterons. However, any ensemble has a symmetry axis $\boldsymbol{S}$ (i.e., is invariant under rotation around $\boldsymbol{S}$), called the *spin alignment axis*. When $\boldsymbol{S}$ is taken as the quantization axis, the relative populations n_+, n_0 and n_- of the magnetic sub-states with $m_s + 1$, 0, or -1, completely define the polarization of the ensemble. For an unpolarized ensemble the sub-states are equally populated ($n_+ = n_0 = n_- = 1/3$). If the $+1$ sub-state is enriched at the expense of the -1 sub-state, the system is said to have *vector* polarization, $P = n_+ - n_-$. If the population n_0 differs from 1/3, the assembly has *tensor* polarization, $P = 1 - 3n_0$. Obviously, the system can be vector- and tensor-polarized at the same time.

With an arbitrary quantization axis, three vector components and five components of a second-rank tensor are required to describe spin-1 polarization, but these so-called beam moments can be deduced if one knows the vector and tensor polarizations, P and P , and the orientation of the spin alignment axis.

1.3.2. *Orbiting polarized deuterons*

The magnetic moment of deuterons is smaller than that of protons ($_d/\mu_p = 0.3070$) and the mass of the deuteron is larger $(m_d/m_p = 1.999)$, so the precession of deuterons is slower, but the spin closed orbit is defined just as it is for protons. Since, for symmetry reasons, the spin alignment axis is collinear with the magnetic moment, the spin closed orbit represents the orientation of $\boldsymbol{S}$, and one can evaluate the beam moments at any point in the ring. The formal treatment of spin-1 particles in a ring has been discussed by Bell [13], and Huang [14].

Since the relevant parameter, $G_d = -0.14299$, is more than an order of magnitude smaller for deuterons than for protons, there are much fewer deuteron depolarizing resonances (the lowest imperfection resonance occurs at 11.3 GeV). There are also fewer intrinsic resonances but they *can* occur at low energy since the tune can be a small number. A polarized deuteron beam has been accelerated and decelerated through an intrinsic resonance at KEK [15]. Very recently, polarized deuterons have been stored at COSY and at IUCF.

1.3.3. *Reversal of deuteron polarization*

In Section 1.2.1, I mentioned the reversal of spin-1/2 polarization by crossing an induced depolarizing resonance. The effect of resonance crossing is related to the crossing speed [4]. Thus, one can compensate for the smaller deuteron magnetic moment by increasing the rf field strength *or* by decreasing the crossing speed. The effect of an induced resonance on a polarized deuteron beam has recently (March 2002) been studied for the first time at the Indiana Cooler [16]. The experiment used a 270 MeV deuteron beam with both, vector and tensor polarization. It was verified that a complete reversal of the spin closed orbit changes the sign of the vector polarization, but does not affect the tensor polarization, as expected. It was also shown that when a resonance is only partly crossed the spin closed orbit may end up in the ring plane when the resonance releases it. Then, the vector polarization vanishes and the tensor polarization is decreased by a factor of two, but has *changed sign*, also as expected [17].

1.3.4. *Vector and tensor polarization lifetime*

Interpreting the depolarization of a stored beam as random walk of the spin closed orbit leads to the prediction of different lifetimes for vector and tensor polarization [17]. A recent experimental test with 270 MeV deuterons near an induced rf solenoid resonance indicates that the vector polarization lifetime is about *twice* that of tensor polarization [16].

2. Polarized, internal targets

2.1. *General remarks*

The attainable production rate by standard methods for atoms with nuclear polarization satisfies the requirements for an internal target. The atomic beam is either crossed with the beam in the ring or injected into a storage cell (see 2.2.1). A guide field over the target region defines the spin alignment axis. If the atoms are in a pure spin state (maximum *total* angular momentum), a weak field of 0.2 0.5 mT, essentially to overcome the earth's field, is sufficient. Corresponding compensating fields can be set up to practically eliminate the effect of transverse guide fields on the beam orbit. A review of polarized internal targets has been given by Rathmann [18].

Polarized internal targets are pure, not susceptible to radiation damage, and offer complete freedom in choosing the direction of the polarization, including rapid reversal of its sign. The ability to use such targets is perhaps the most

important benefit of the storage ring environment for nuclear physics.

Until recently, it was assumed that atoms that recombine into molecules lose their polarization. However, it has been demonstrated by a study at the Indiana Cooler [19] that H_2 molecules may well retain some nuclear polarization.

At high atomic density, when mixed hyperfine states are present, their populations are modified by spin-exchange collisions, reducing the resulting nuclear polarization [20].

2.2. *Technical realization*

2.2.1. *Storage cells*

For a given flux of polarized atoms, the target thickness can be enhanced by several orders of magnitude by directing the atomic beam from the side into a narrow, open-ended channel through which the stored beam passes. The purpose of such a so-called storage cell is to provide gas flow impedance. This scheme was first used at the VEPP-3 electron storage ring in Novosibirsk [21]. To avoid depolarization of the atoms by wall collisions, the cell walls are coated with Teflon, dri-film, frozen water, or some other material [22]. The conflicting criteria that enter the design of a storage cell target are discussed in Ref. [23].

2.2.2. *Sources of polarized atoms*

The preferred method to produce polarized H and D atoms is to dissociate the molecules, form a beam and then select a single hyperfine state or a desired mixture of states. This selection is affected by a combination of sextupole fields (to discard one electron sub-state) with rf-induced transitions between magnetic sub-states. It is possible to generate pure deuteron vector or pure tensor polarization. The Wisconsin atomic-beam source [24] that is in use at the Indiana Cooler, generates a beam of about 1 cm diameter, suitable for injection into a storage cell, with a flux of about 3 10^{16} polarized H atoms/s with nuclear polarization $P = 0.75$. For a typical storage cell of 1 cm diameter and 25 cm length, the target thickness then amounts to between 10^{13} and 10^{14} atoms/cm^2.

An alternative method to produce polarized atoms makes use of spin exchange between H (or D) atoms and a small admixture of optically pumped potassium atoms [25]. This method produces a higher flux, but (so far) quite low nuclear polarization. This and the unavoidable potassium contamination of the target are serious disadvantages of this method.

Polarized ^{3}He is obtained by producing meta-stable atoms by optically pumping the $^3S_1 - ^3P_0$ transition, and then transferring the nuclear polarization by "metastability exchange" collisions to the ground state. A flow into the storage cell of 10^{17} atoms/s with a polarization of $P = 0.4$ has been reported [26].

3. Nucleon–Nucleon reactions

3.1. *Proton–proton elastic scattering*

3.1.1. *What can be measured? (spin-1/2 on spin-1/2 with a two-particle final state)*

The beam polarization as well as the target polarization may have non-zero components along the axes of a fixed Cartesian frame. Either beam or target or both may also be unpolarized. Thus, there are 16 combinations of beam and target polarization states, each of which corresponds to an observable. These observables include the unpolarized cross section $_{00}$, the analyzing powers A_{i0} and A_{0k} and the spin correlation coefficients C_{ik} (i and k stand for x, y, or z, where the z-axis is along the beam, the y-axis is up, and the x-axis completes a right-handed coordinate frame). Four of these observables are related to others by a simple rotation of the frame around the beam axis (e.g., C_{xz}, rotated by 90 is the same as C_{yz}). Another four observables vanish if parity is conserved. The remaining seven observables are the beam and the target analyzing power, A_{y0} and A_{0y}, and the correlation coefficients C_{xx}, C_{yy}, C_{zz}, C_{xz} and C_{zx}. Each of these is a function of the polar angle and the azimuth φ. The dependence on may be complicated (depending on the number of participating partial waves), but the φ dependences are a simple trigonometric functions. Each observable is associated with a known, characteristic φ dependence. This dependence is crucial in distinguishing observables from each other when analyzing the data. For this reason, it helps to have a detector with full azimuthal coverage. Ohlsen [27] has given a complete treatment of the formal aspects of spin correlation measurements.

If the particles in the initial state are both protons, two of the seven observables listed above become redundant (A_{0y} and C_{zx} are equivalent to A_{y0} and C_{xz}) due to the identity of the collision partners.

3.1.2. *$p + p$ elastic scattering at IUCF and COSY*

A fair number of experiments with the Indiana Cooler were aimed at the analyzing power A_y and three of the four spin correlation coefficients, C_{xx}, C_{yy}, C_{xz} (in pp scattering, often called A_{xx}, A_{yy}, A_{xz}, or A_{SS}, A_{NN}, A_{SL}). Initial measurements near 200 MeV [28–31] were accompanied by the development of the new technology and novel analysis tools [32]. Finally, a general survey of these observables from 200 to 450 MeV [33], using up- and down-ramping to export the polarization calibration, resulted in an impressive body of data with statistical uncertainties of about 0.01 and an overall normalization error of 2.4%. A measurement of the fourth correlation coefficient, C_{zz}, at 200 MeV [34] made use of a solenoid snake to generate beam with longitudinal polarization at the target.

The EDDA collaboration at COSY subsequently continued these measurements to higher energies, resulting in analyzing power and spin correlation coefficients between 450 MeV and 2.5 GeV. A noteworthy achievement was that continuous excitation functions were obtained by taking data *while* the beam was accelerated [35].

3.1.3. *Physics interest: NN phenomenology*

The high precision of the data, and the fact that the clean definition of the scattering events made the small angles of the Coulomb-nuclear interference region accessible, made it possible to demonstrate, for the first time, a significant effect due to the interaction of the magnetic moments. However, a more important consequence of the Indiana data was that they required an update of the phenomenological description of *NN* scattering in terms of empirical phase shifts. This is even truer at GeV energies where the

new COSY data had a significant impact on the pp phase shift analysis in this energy range [36]. The NN phase shifts constitute the basis for numerous models in nuclear physics.

3.2. *Meson production in p + p collisions*

3.2.1. *What can be measured? (spin-1/2 on spin-1/2 with a three-particle final state)*

Compared to a two-particle final state, we need to specify a third momentum vector to describe the final-state kinematics. This brings the number of kinematic variables to a total of five. These can be $_1$, φ_1 (direction of particle 1, e.g., the pion), $_{23}$, φ_{23} (direction of the relative momentum between particle 2 and 3, e.g., the two nucleons), and ε (energy sharing between the three particles). Again the azimuthal dependences are predictable and useful for data analysis. Thus, the seven observables defined for the two-body case (Section 3.1.1) are now five-dimensional ($_1$, $_{23}$, φ_1, φ_{23}, ε). One can reduce this information systematically into a (fairly large) set of one-dimensional quantities by integrating either over $_{23}$ and ε, or over $_1$ and ε [37].

But this is not all. Since in a three-body final state parity conservation no longer constrains any observables, we must now also consider the longitudinal analyzing powers A_{z0} and A_{0z}, and the correlation coefficient $C_{xy} - C_{yx}$. In addition, one must address the dependence on the energy-sharing parameter ε (for instance, by studying the dependence on ε of the unpolarized cross section and the spin-dependent total cross sections $\Delta\ _T$ and $\Delta\ _L$). The formal aspects of polarization observables in reactions with a three-particle final state are treated in detail in Ref. [37].

3.2.2. *Physics issues*

In meson production near threshold relatively few partial waves contribute. For the reaction pp $\rightarrow$ pp ^{0}, up to about 400 MeV bombarding energy, the final-state angular momenta of the two nucleons (L_{NN}) and of the pion (ℓ) are both either 0 or 1, and within the first 20 MeV above threshold just a *single* partial wave $\left({}^3\mathrm{P_o} \rightarrow {}^1\mathrm{S_o}(\ell = 0)\right)$ is important. Early pion-production experiments in this energy region yielded the first evidence for the importance of heavy meson exchange [38] and the associated enhancement of the axial current in a nuclear system. But the theoretical situation is far from settled, since other contributions (such as off-shell pion rescattering) may also be relevant. A meaningful test of models, at this stage, needs more that just the strength of the $L_{NN} = \ell = 0$ amplitude. Such information is provided by polarization observables.

3.2.3. *Pion production experiments at the Indiana Cooler*

The first pion production polarization experiments at the Cooler were measurements near threshold of cross section and analyzing power for the reactions pp $\rightarrow$ d $^+$ [39] and pp $\rightarrow$ pn $^+$ [40,41]. After the polarized internal target became available, a program to study spin correlation in pp $\rightarrow$ pp ^{0} was initiated [42,43], and it was demonstrated that model-independent information on the contribution of a single partial-wave amplitude can be deduced from the spin-dependent cross sections $\Delta\ _T$ and $\Delta\ _L$ alone [44]. This effort eventually led to a complete measurement of all observables of pp $\rightarrow$ pp ^{0} with polarization in the initial state, everywhere in the three-body phase space, up to 400 MeV [37]. This data set provides sufficient information to experimentally determine all 12 amplitudes for which L_{NN} and ℓ are either 0 or 1.

Perhaps the single most interesting result was the observation that the longitudinal analyzing power A_z (normally forbidden by parity conservation) can well be large in a reaction with a three-body final state [45]. Concurrently with the pp $\rightarrow$ pp ^{0} experiment, data on the spin correlation coefficients in pp $\rightarrow$ d $^+$ [46] and in pp $\rightarrow$ pn $^+$ [47,48] were also obtained.

3.2.4. *Meson production at COSY*

At COSY, the first polarization data in meson production begin to emerge: very recently the COSY-11 collaboration has reported a measurement of the analyzing power (with respect to the meson) of pp $\rightarrow$ ppη, 40 MeV above threshold [49].

4. *P + D* reactions below the pion threshold

4.1. *Proton–deuteron elastic scattering*

4.1.1. *What can be measured? (spin-1/2 on spin-1 with a two-particle final state)*

When the spin-1 particles are *vector*-polarized, the situation is analogous to the spin-1/2 on spin-1/2 case: there are a total of seven observables, namely two analyzing powers and five 'vector' spin correlation coefficients.

For *tensor*-polarized spin-1 particles (see Section 1.3.1) there is some added complexity. Good introductions to tensor observables, terminology and conventions are given, e.g., by Haeberli [50], and Darden [51].

In Cartesian notation, a tensor-polarized beam (or target) has five independent moments, p_{xx}, p_{xy}, p_{xz}, p_{yy} and p_{yz} (p_{zz} is not independent because $p_{xx} + p_{yy} + p_{zz} = 0$). There are 20 ways to combine these with the four possibilities for the spin-1/2 particle (indices 0, x, y, z). Of these combinations, seven are related to others by rotation around the beam axis, and three are forbidden by parity conservation. The remaining observables are the three tensor analyzing powers A_{xx}, A_{yy} and A_{xz}, and the seven 'tensor' correlation coefficients $C_{xx,y}$, $C_{xy,x}$, $C_{xy,z}$, $C_{xz,y}$, $C_{xz,z}$, $C_{yy,y}$ and $C_{yz,x}$. Thus, apart from the unpolarized cross section, there are a total of 17 polarization observables that can be measured in p + d elastic scattering with polarized collision partners (for a formal discussion of spin correlation measurements, see Ohlsen [27]).

4.1.2. *Polarization data for p + d scattering*

A number of measurements of the proton analyzing power, and the deuteron vector and tensor analyzing powers exist between proton bombarding energies between 100 and 200 MeV (see references given in Ref. [52]). The first spin correlation measurement $\left(C_{y,y}\right)$, together with the deuteron vector analyzing power, has been carried out at 200 MeV [53] at the Indiana Cooler, using a laser-driven polarized target. More recently, the PINTEX group has embarked on a program to measure all but two of the 17 possible polarization observables. This experiment has been carried out at two beam energies (135 and 200 MeV stored,

polarized protons including longitudinal polarization) and an atomic-beam deuterium target with either pure vector or pure tensor polarization. The analysis of these data is in progress; preliminary results from a subset of the data are in hand.

4.1.3. *Physics interest: the three-nucleon force*

It is believed that today's state-of-the-art Faddeev calculations, solving the three-nucleon problem with a phenomenological *NN* input, are telling us how nature would behave if there were only two-nucleon forces. It has been shown that these calculations depend only weakly on the choice of the underlying NN potential. They neglect the Coulomb force but there is evidence that this does not matter above 100 MeV and for $_{\mathrm{cms}} > 30$. Comparing such calculations with a complete set of polarization data thus promises to reveal information about the three-nucleon force, in particular its spin dependence.

The general features of our preliminary $p + d$ elastic scattering results are reproduced rather well by the most recent 2N Faddeev calculations [54]. The remaining discrepancies are most pronounced for center-of-mass angles greater than 70 and forward of 30 (the latter presumably because of Coulomb effects). The observables with the largest discrepancies are the tensor analyzing powers. Inclusion of either the Tucson–Melbourne 3NF or the Argonne IX three-nucleon force often (but not always) reduces the discrepancy. Clearly, much more theoretical work is needed to *quantitatively* explain the disparity between experiment and 2NF calculations. It may also be worthwhile to search for a *phenomenological* three-nucleon potential that would explain the data, much along the lines of the phenomenological potentials that we employ to describe the NN interaction.

4.2. *Deuteron break-up reaction*

4.2.1. *Physics issue: axial observables*

When searching for 3NF effects, the break-up into three nucleons has an advantage since the kinematic freedom in the final-state offers the possibility to select configurations, which differ in their sensitivity to 3N forces. For instance, 3NF effects predicted for spin correlation observables by the Tucson–Melbourne force are negligible near the quasi-free peak, but are quite large in the "FSI" configuration where two of the outgoing nucleons are at relative rest [55].

On the other hand the complexity of the spin-1/2–spin-1 spin space combined with a three-body phase space is mind-boggling, and a measurement clearly needs some guidance. Such guidance is provided, for instance, by the following argument.

It was pointed out by Knutson [56] that three-body potentials involve spin operators of a type that is not allowed for ordinary two-body interactions. These operators affect the so-called "axial" observables. An example of an axial observable is the longitudinal analyzing power A_z. In reactions with two outgoing particles this observable must vanish by parity conservation, but it is unconstrained when there are outgoing particles with lab momenta that are not co-planar.

An attempt to observe a non-zero A_z in pd $\rightarrow$ ppn with a longitudinally polarized 9 MeV proton beam [57] failed (an upper limit of 0.003 was established, in agreement with Faddeev predictions). Somewhat surprisingly, the same calculations at 135 MeV predict a much larger value for A_z. This opens up the exciting possibility of an experiment that addresses the 3NF where the choice of the quantity to be measured is motivated by a theoretical argument.

4.2.2. *Measurement of A_z at 135 MeV*

One of the last experiments with the Indiana Cooler (ce64) aims at a measurement of A_z in pd$\rightarrow$ppn at 135 MeV (proton energy). The experiment is carried out with a 270 MeV deuteron beam on a proton target. Even though the focus is the longitudinal analyzing power, vector- and tensor-polarized beam is used and the target polarization is not just pointed along the z-axis but also along the x- and the y-axis. Thus, given the interest and the manpower, much more than A_z could be extracted from the data. The data taking is completed. From a first look at the data, it is evident that the observed A_z is indeed sizeable.

5. More few-nucleon reactions

5.1. *Pion production in $p + d$ collisions*

5.1.1. *What can be measured? (spin-1/2 on spin-1 with a three-particle final state)*

Combining the complexity of spin-1/2 on spin-1 with a five-parameter three-body phase space results in an overwhelming number of polarization observables, making a complete study a monumental task. Let me therefore discuss here just the spin-dependent total cross section, which has relatively few terms. To measure the total cross section, we integrate over all degrees of freedom of the final state by having a detector that covers all (or, most) of phase space. Then, there are only *four* polarization observables left, namely the tensor analyzing power A_{zz} (no spin-1/2 polarization), integrated over phase space, two spin-dependent total cross sections $\Delta\ _T$ and $\Delta\ _L$ measured with vector polarized spin-1 particles, and the integrated tensor correlation coefficient $C_{yz,x} - C_{xz,y}$.

5.1.2. *Physics issues*

Pion production in the three-nucleon system is interesting because it represents the simplest case where one may study the effect of the 'medium' (actually, one more nucleon) on the production of mesons. The nuclear wave functions of the three-nucleon system are presumably under control. Nevertheless, microscopic calculations have not been very successful explaining the cross section and even less the available polarization data. For this reason, a number of theoretical studies attempted to describe p + d pion production in terms of the amplitudes of the underlying elementary process $NN \rightarrow$ d (see, e.g., [58] and references therein). Spin-correlation data (e.g., a measurement of $\Delta\ _T$ and $\Delta\ _L$), would provide model-independent information on the importance of different reaction mechanisms.

Based on qualitative agreement with the pd $\rightarrow$ t $^+$ cross section at 800 MeV it has been argued that mechanisms involving all three nucleons are important [59]. This offers some hope that eventually information about the three-nucleon force might also be obtained from pion production in the three-nucleon system.

5.1.3. *Polarization measurements*

Below 500 MeV, the proton analyzing power and vector- and tensor analyzing powers have been measured for pd $\rightarrow {}^3$He ^{0} before the advent of storage rings. At the Indiana Cooler the proton analyzing power for pd $\rightarrow {}^3$He ^{0} has been measured at energies from 199.4 to 210 MeV [60]. More recently, also at the Cooler, the first spin correlation data have been obtained for the reaction pd $\rightarrow$ t ^{4}. In this experiment the spin-dependent total cross sections Δ_T and Δ_L were measured at 250 and 275 MeV. The analysis of this experiment is in progress.

5.2. *$p + d$ reactions at GeV energies*

5.2.1. *$p + d$ break-up*

As the bombarding energy increases beyond the pion threshold, Faddeev calculations can not yet be used to describe the three-nucleon continuum. On the other hand, one might hope that few-nucleon reactions get simpler as the energy is increased. However, this does not deem to be the case, given the very limited success of the impulse approximation to describe, e.g., p + d break-up. We are thus relegated to models, evaluating contributions from various postulated reaction mechanisms. Selective tests of such models make use of a specific choice of the final-state kinematics, and of the observation of polarization observables. Recently, the ANKE experiment at COSY has measured the analyzing power of pd break-up with a proton pair with low relative energy (presumably in a $^1S_0$ state) in the final state [49]. Eventually, these experiments will also cover spin-correlation observables.

5.2.2. *$p + d$ total cross section: time reversal invariance*

It is commonly thought that many of the systematic errors that make the classical tests for charge symmetry, parity violation and time reversal invariance hard, are easier to handle in a storage ring environment. Yet such experiments are slow in coming. Here, I would like to mention one experiment that probably can only be done in a storage ring.

In Section 5.1.1 I have discussed the total cross section of the p + d reaction. One of the contributions to the spin-dependence of the total cross section, the tensor correlation coefficient $C_{yz,x} - C_{xz,y}$, can be shown to vanish under time reversal if one includes all exit channels (but only then) [61]. There exists a proposal to exploit this observable for a time reversal invariance test at COSY [62], using a vertically polarized proton beam and a tensor-polarized, internal deuteron target. A similar experiment at very high energy has also been discussed for RHIC.

5.3. *Spin-dependence of bound-state wave functions*

5.3.1. *Physics issues*

Many experimental queries in nuclear physics, from $NN \rightarrow X$ reactions, to studies of parton polarization with high-energy electrons at JLAB and HERA, to polarization studies at very high energy at RHIC, require polarized neutrons as collision partners. This can be achieved by using the neutrons in polarized D or ^{3}He nuclei. Neutrons in vector-polarized deuterons are polarized in the same direction, except for the d-state where the neutron polarization is opposite. Similarly, the unpaired neutron and a singlet np pair, except for admixtures of other configurations, give the ^{3}He He polarization. Thus, such measurements with polarized neutrons require knowledge of the spin-dependent nuclear wave functions, and a model is needed to determine the effective nucleon polarization under the kinematic constraints of the experiment in question. Spin correlation measurents can test such models.

5.3.2. *Spin correlation in quasi-free $p + {}^3He$ scattering*

The difference between the single-nucleon momentum-density distributions with the nucleon spin parallel or anti-parallel to the ^{3}He spin has been studied at the Indiana Cooler. To this effect, the spin correlation coefficients for quasi-elastic np or pp scattering were measured with a polarized proton beam on an internal ^{3}He target, polarized by optical pumping [63]. The data were analyzed assuming the validity of the plane-wave impulse approximation [64] and good agreement with theoretical models of ^{3}He was found up to about 300 MeV/c Fermi momentum.

6. Summary and outlook

The first measurement with a polarized beam in the Indiana Cooler (see Fig. 1) took place in 1988, and the first polarized internal target (^{3}He) was in use by 1994. Most of the storage ring experiments with polarized hadrons to date, and much of the development of the associated technology, were carried out at Indiana. This article has been an attempt to summarize this work.

As of this year, the "Cooler" is no more. The future in polarization studies at a storage ring belongs to COSY. The only other storage ring in the world that features polarized, hadronic collision partners is RHIC, where very different physics questions will be investigated using many of the techniques and methods developed and first tested at IUCF.

References

1. Montague, B. W., Phys. Rep. **113**, 1 (1984).
2. Rathmann, F. *et al.*, Phys. Rev. Lett. **71**, 1379 (1993).
3. Meyer, H. O., Phys. Rev. **E50**, 1485 (1994).
4. Caussyn, D. D. *et al.*, Phys. Rev. Lett. **73,** 2857 (1994).
5. Przewoski, B. v. *et al.*, Rev. Sci. Instr. **67,** 165 (1996).
6. Blinov, B. B. *et al.*, Phys. Rev. Lett. **88**, 014801–1 (2002).
7. Meyer, H. O. *et al.*, Phys. Rev. **E56**, 3578 (1997).
8. Przewoski, B. v. *et al.*, Rev. Sci. Instr. **69**, 3146 (1998).
9. Pollock, R. E. *et al.*, Phys. Rev. **E55**, 7606 (1997).
10. Crandell, D. A. *et al.*, Phys. Rev. Lett. **77**, 1763 (1996).
11. Krisch, A. D. *et al.*, Phys. Rev. Lett. **63**, 1137 (1989).
12. Goodwin, J. E. *et al.*, Phys. Rev. Lett. **64**, 2779 (1990).
13. Bell, J. S., CERN yellow report **75–11** (available from CERN via the Web).
14. Huang, H., Lee, S. Y. and Ratner, L., Proc. Particle Accelerator Conf., Washington, DC, 1993, IEEE, p. 432.
15. Sato, H. *et al.*, Nucl. Instr. Meth. **A385,** 391 (1997).
16. Krisch, A. D. *et al.*, Indiana Cooler exp. Ce83, March 2002.
17. Meyer, H. O., Nucl. Phys. **A631**, 122c (1998).
18. Rathmann, F., Proc. 9th Int. Workshop on Polarized Sources and Targets (PST2001), (eds. Derenchuk, V. P. and Przewoski, B. v.) World Scientific, Singapore, 2002, p. 3.
19. Wise, T. *et al.*, Phys. Rev. Lett. **87**, 042701 (2001).
20. Walker, T. and Anderson, L. W., Nucl. Instr. Meth. **A334**, 313 (1993).
21. Gilman, R. *et al.*, Phys. Rev. Lett. **14**, 1733 (1990).
22. Price, J. S. and Haeberli, W., Nucl. Instr. Meth. **A349**, 321 (1994).

23. Meyer, H. O., Proc. Int. Workshop on Polarized Beams and Polarized Gas Targets, (eds. Paetz, H., gen. Schiek and Sydow, L.) (Cologne, Germany, June 1995), (World Scientific, Singapore, 1996), p. 355.
24. Wise, T., Roberts, A. D. and Haeberli, W., Nucl. Instr. Meth. **A336**, 410 (1993).
25. Coulter, K. P. *et al.*, Phys. Rev Lett. **68**, 174 (1992).
26. Bloch, C. *et al.*, Nucl. Instr. Meth. **A354**, 437 (1995).
27. Ohlsen, G. G., Rep. Prog. Phys. **35**, 717 (1972).
28. Pitts, W. K. *et al.*, Phys. Rev. **C45**, R1 (1992).
29. Pitts, W. K., Phys. Rev. **C45**, 455 (1992).
30. Haeberli, W. *et al.*, Phys. Rev. **C55**, 597 (1997).
31. Rathmann, F. *et al.*, Phys. Rev. **C58**, 658 (1998).
32. Meyer, H. O., Phys. Rev. **C56**, 2074 (1997).
33. Przewoski, B. v. *et al.*, Phys. Rev. **C58**, 1897 (1998).
34. Lorentz, B. *et al.*, Phys. Rev. **C61**, 054002 (2000).
35. Altmeier, M. *et al.*, Nucl. Instr. Meth. **A431**, 428 (1999).
36. Altmeier, M. *et al.*, Phys. Rev. Lett. **85**, 1819 (2000).
37. Meyer, H. O. *et al.*, Phys. Rev. **C63**, 064002 (2001).
38. Lee, T. S. H. and Riska, D. O., Phys. Rev. Lett. **70,** 2237 (1993).
39. Heimberg, P. *et al.*, Phys. Rev. Lett. **77**, 1012 (1996).
40. Daehnick, W. W. *et al.*, Phys. Lett. **B423**, 213 (1998).
41. Flammang, R. W. *et al.*, Phys. Rev. **C58**, 916 (1998).
42. Rinckel, T. *et al.*, Nucl. Instr. Meth. **A439**, 117 (2000).
43. Meyer, H. O. *et al.*, Phys. Rev. Lett. **81**, 3096 (1998).
44. Meyer, H. O. *et al.*, Phys. Rev. Lett. **83**, 5439 (1999).
45. Meyer, H. O. *et al.*, Phys. Lett. **B480**, 7 (2000).
46. Przewoski, B. v. *et al.*, Phys. Rev. **C61**, 064604 (2000).
47. Swapan, K. Saha, *et al.*, Phys. Lett. **B461**, 175 (1999).
48. Daehnick, W. W. *et al.*, Phys. Rev. **C65**, 024003 (2002).
49. COSY Annual Report 2001, Forschungszentrum Julich (2002).
50. Haeberli, W., "Nucl. Spectrosopy and Reactions," Part A, (ed. Cerny) (Academic Press, NY, 1974) p. 151.
51. Darden, S. E., in Proc. 3rd Int. Symp. on Polarization Phenomena in Nuclear Reactions, (eds. Barschall, H. H. and Haeberli, W.), (University of Wisconsin Press, Madison, 1971), p. 39.
52. Meyer, H. O., Proc. 8th Conf. on Mesons and Light Nuclei, Prague, Czech Republic, (ed. Adam, J., Bydzovsky, P. and Mares, J.), AIP Conf. Proc. v.603 (2001), p. 113.
53. Cadman, R. V. *et al.*, Phys. Rev. Lett. **86**, 967 (2001).
54. Witala, H. *et al.*, Phys. Rev. **C63**, 024007 (2001).
55. Glockle, W., Witala, H., Huber, D., Kamada, H. and Golak, J., Phys Rep. **274**, 107 (1996).
56. Knutson, L. D., Phys. Rev. Lett. **23**, 3062 (1994).
57. George, E. A. *et al.*, Phys. Rev. **C54**, 1523 (1996).
58. Falk, W. R., Phys. Rev. **C61**, 034005 (2000).
59. Laget, J. M. and LeCollet, J. F., Phys. Lett. **B194**, 177 (1987).
60. Warman, L. K., Ph.D. thesis, Indiana University, 1998 (experiment ce58).
61. Conzett, H. E., Phys. Rev. **C48**, 423 (1993).
62. Eversheim, P. D., Proc. 4th Int. Conf., Bloomington, IN, September 1999, (eds. Meyer, H. O. and Schwandt, P.), API Conference Proceedings **512**, (Am. Inst. of Physics, New York, 2000).
63. Miller, M. A. *et al.*, Phys. Rev. Lett. **74**, 502 (1995).
64. Milner, R. G. *et al.*, Phys. Lett. **B379**, 67 (1996).

Author Please resupply Fig. 1 if quality not good enough